Recent Developments in Electronics and Communication Systems
KVS Ramachandra Murthy et al. (Eds.)

doi:10.3233/ATDE221335

Wave Spectral Analysis of Visakhapatnam Port Under the Resonance Conditions

Prachi Priya[a], Prashant Kumar[a,1] and Rajni[b]
[a] *Department of Applied Sciences, National Institute of Technology Delhi, Delhi-110040*
[b] *Jindal Global Business School, O P Jindal Global University Sonipat, Haryana-131001*

ORCiD ID:
Prashant Kumar : https://orcid.org/0000-0001-8480-7490
Rajni https://orcid.org/0000-0002-7187-6363

Abstract. The Visakhapatnam port, India is a major natural port, situated in between the Kolkata and Chennai on the East Coast and in terms of latitude and longitude its location is 17.6856° N, 83.2160° E has experienced an extreme wave oscillations 2.0 to 6.0 m in the midst of its severe weather events. In this paper numerical studies are performed to analyze the frequency distribution over the oceanic surface of standing waves in Visakhapatnam port at four respective synthetic record stations in presence of partially reflecting harbor. The convergence study is conducted to obtain the numerical accuracy of the scheme and simulation results are validated with the available studies experimentally from Ippen and Goda (1963) and Lee (1971) also with the analytical approximations. Further, the spectral density is determined corresponding to the wave period for the incident waves striking with several directions towards the Visakhapatnam port at four different record stations. The computation of the resonant frequencies is conducted in the Visakhapatnam port to examine the safe locations for the moored ship. Abstract goes here.

Keywords. Boundary Element Method, Amplification Factor, Spectral Density, Helmholtz Equation, Reflection Coefficient, Visakhapatnam Port

1. Introduction

The extreme waves cause wave hazards involving tropical storms, cyclones, tsunamis, etc. which is difficult to handle and may persist for many days, resulting lots of destruction on the coastal region and damages on the coastal structures like harbor, fenders, mooring ropes and also disturbs the unloading and loading cargo phenomenon on the moored ship. Visakhapatnam port, India is one of the major ports in India which provides significant contribution in trade with countries like Japan, China, Australia and many more European and Asian countries. It also serves in industries like SAIL, HPCL, NLCO, and others in Andhra Pradesh, India, as well as other states such as Maharashtra, Odisha, Jharkhand, Chhattisgarh, Madhya Pradesh, and Telangana. A total of approx. 126 million tons of cargo handled per year.

[1] Corresponding Author: Prashant Kumar, prashantkumar@nitdelhi.ac.in

The study of wave oscillations considering constant depth on the defined geometry like circular domain [1], rectangular domain [2] and on two interconnected rectangular basins ([3] and [4]). To study the wave oscillations on complex geometry of port leads to development of various numerical methods like Boundary Element Method (BEM) ([5], [6], [7] and [8]), Hybrid Finite-Element method (HFEM) [9], Finite-Element Method (FEM) [10]. Further, the study also includes the nonlinear waves on harbor by Guerrini [11] using Boussinesq equation, wave analysis for low frequency by Dong [12], for short wave Gao [13] with the consideration of fringing reefs [14], and for high resonance mode [15]. The numerical study applied on the realistic harbor by various researchers, Long beach harbor in California, USA ([5] and [16]), Hua-Lien Harbor in Taiwan [17], Marina de Ferrol in Spain [18], Paradip Port [8], and by Dong [19] on Hambantota Port The studies mentioned above are accurate and efficient, coastal engineers can use them to strengthen coastal structures and utilized to redesign the harbour model based on resonance mode analysis in the harbour domain.

In this paper, the study of spectrum analysis within the Visakhapatnam port is analyzed by using the Mitsuyasu's spectrum [20] for the multidirectional random waves. This numerical scheme based on the well-known Boundary element method which is utilized to solve the Helmholtz equation including partially reflecting harbor boundary. The convergence and comparisons are presented to verify the scheme and the wave characteristic inside the Visakhapatnam port through spectral density are discussed at four record station to examine the safe place for moored ship.

2. Mathematical Formulation

The Visakhapatnam port geometry is presented in Figure 1. The global Cartesian co-coordinate system (x, y, z) is taken where x-co-ordinate represents the direction of wave propagation, y-co-ordinate is along unbounded sea region whereas z-co-ordinate in the vertical direction along the depth of ocean. The total fluid domain is divided into two major regions, Region-I (unbounded region) and Region-II (bounded region) and both regions are connected with entrance AB $\left(\Gamma_e\right)$ and the bounded region is surrounded with partially reflecting boundary. The incident wave diffracted and refracted inside the port through entrance.

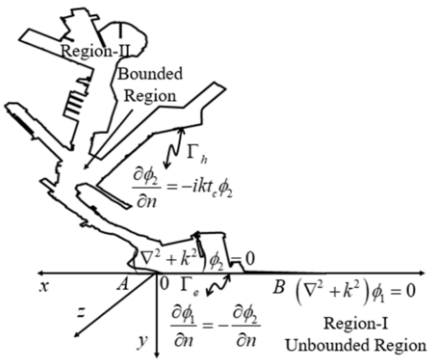

Figure 1. Sketch of Visakhapatnam port model formulation, including the governing equations and various boundary conditions in Region-I (unbounded) and Region-II (bounded).

2.1. Wave Function in Bounded and Unbounded Region

There is presumed that the fluid to be incompressible, inviscid and the motion of fluid is irrotational hence from potential flow theory the potential function satisfy the Laplace equation and for constant depth continuity equation is used to obtain the Helmholtz equation for both the regions (Region-I and Region-II) and the solution of wave function follows

$$\left(\nabla^2 + k^2\right)\phi_i = 0, \qquad i = 1,2 \tag{1}$$

where i = 1, 2 represents the wave function for unbounded and bounded region respectively and the following boundary conditions are imposed on the fluid domain

$$\frac{\partial \phi_i}{\partial z} - \frac{\omega^2 \phi_i}{g} = 0, \quad i = 1,2 \text{ on free surface} \tag{2}$$

$$\frac{\partial \phi_i}{\partial n} = 0, \qquad i = 1,2 \qquad \text{on bottom surface} \tag{3}$$

$$\frac{\partial \phi_2}{\partial n} = it_c k \phi_2 \qquad \text{on } \Gamma_h \tag{4}$$

where t_c complex transmission coefficient and in terms of reflection coefficient R_c

$$\mathrm{Re}\left(t_c\right) = 0 \text{ and } \mathrm{Im}\left(t_c\right) = \frac{1 - R_c}{1 + R_c} \tag{5}$$

In Region-I, the wave function satisfies the radiation condition at infinity to ensure wave propagates outward

$$\lim_{R\to\infty} \sqrt{R}\left(\frac{\partial \phi_{rad}}{\partial R} - ik\phi_{rad}\right) = 0, \qquad R = x^2 + y^2 \tag{6}$$

At the entrance AB where the unbounded region connected with bounded region, the continuity conditions are implemented to verify the continuation of velocity and pressure and is defined as

$$\phi_1 = \phi_2 \text{ and } \frac{\partial \phi_1}{\partial n} = -\frac{\partial \phi_2}{\partial n} \tag{7}$$

The Helmholtz equation in the bounded region is transformed into an integral equation along the boundary of the domain and the solution follows the Green's identity theorem and written as

$$\phi_2\left(\vec{x}_i\right) = C\int_S \left[\phi_2 \frac{\partial H_0^1\left(kr\right)}{\partial n} - H_0^1\left(kr\right)\frac{\partial \phi_2}{\partial n}\right] dS\,, \qquad S = \Gamma_e \cup \Gamma_h \tag{8}$$

where, $C = \begin{cases} 1/4i & \text{at any interior points,} \\ 1/2i & \text{at bondary points.} \end{cases}$ and $H_0^1\left(kr\right)$ is the Hankel function of first kind and zero order.

The boundary of the port region, which consists of the shoreline of the port and entrance boundary is discretize into N number of finite segments and from Eq. (8) the Region-II is written as a matrix form as

$$\left[\phi_2\left(\vec{x}\right)\right] = [M][X] \tag{9}$$

where, $[M]_{N\times N}=\left[\left[[Gn]+\left[U_0\right][G]-[I]\right]^{-1}[G]\right]_{N\times N}\left[U_1\right]_{N\times N_e}$,

$[Gn]_{N\times N}=\left[C\frac{\partial}{\partial n}\left(H_0^1\left(kr_{ij}\right)\right)\Delta s_j\right]$, $[G]_{N\times N}=\left[CH_0^1\left(kr_{ij}\right)\Delta s_j\right]$, $[U_0]=ikt_c\begin{bmatrix}0\\ I_{N_h\times N_h}\end{bmatrix}_{N\times N}$,

$[U_1]=ikt_c\begin{bmatrix}I_{N_e\times N_e}\\ 0\end{bmatrix}_{N\times N_e}$, $[X]_{N_e\times 1}=\left[\frac{\partial}{\partial n}\left(\phi_2\left(\vec{x}_j\right)\right)\right]$.

The solution of Helmholtz equation in Region-I comprise of sum of an incident, reflected and radiated wave and the solution of radiated wave function ϕ_{rad} for Region-I is

$$\phi_{rad}\left(\vec{x}\right)=C\int_{\Gamma_e}\left[\phi_{rad}\frac{\partial}{\partial n}\left(H_0^1\left(kr\right)\right)-H_0^1\left(kr\right)\frac{\partial}{\partial n}\left(\phi_{rad}\right)\right]dS \tag{10}$$

The boundary of the unbounded region which consists of entrance boundary is discretise into N_e number of finite segments and thus solution of wave function in Region-I is in matrix form

$$\left[\phi_1\right]_{N_e\times 1}=\left[\phi_{inc}+\phi_{ref}\right]+[G]\left[[X]+\left[\frac{\partial\phi_{inc}}{\partial n}+\frac{\partial\phi_{ref}}{\partial n}\right]\right] \tag{11}$$

Applying the continuity condition Eq. (7) at common boundary *AB*, of the wave function at the entrance (*AB*) is obtained and then the wave function at any place inside the bounded domain as well as wave amplification is also calculated inside/outside the harbor domain.

2.2. Spectral Density

The spectral density represents the distributions of frequencies over the ocean surface, i.e. which frequencies shows the strong variations and which frequencies shows the weak variations. The spectral density function is calculated with the help of an efficient numerical method Fast Fourier transformation (FFT) for Discreate Fourier transformation (DFT). The directional spectral density $S(f, \theta_{inc})$ is defined as the product of dimensionless multidirectional spreading function $E(f, \theta inc)$ and a multi-directional frequency spectrum $S(f)$

$$S\left(f,\theta_{inc}\right)=E\left(f,\theta_{inc}\right)S\left(f\right) \tag{12}$$

The $S(f)$ and $E(f, \theta inc)$ are defined as

$$S\left(f\right)=0.258\frac{H_s^2}{T_s^4}f^{-5}e^{-1.03(T_sf)^{-4}}\text{ and}$$

$$E\left(f,\theta_{inc}\right)=\frac{1}{2\pi}2^{2s-1}\frac{\Gamma^2\left(s+1\right)}{\Gamma\left(2s+1\right)}\cos^{2s}\left(\frac{\theta_{inc}-\theta_0}{2}\right) \tag{13}$$

where, H_s and T_s represents the wave height and wave period respectively with the principle direction of incident wave denoted by θ_0.

3. Convergence Analysis

The current numerical scheme's order of convergence is determined for the rectangular port by using least square method by dividing the port into N_1, N_2, N_3,… number of segments. For i =1, 2 the error norm is as follows

$$E_{N_i} = \left\| \phi_{N_i}\left(\vec{x}\right) - \phi_{N_t}\left(\vec{x}\right) \right\|_2 = \frac{c}{N_i^{\theta}} \qquad ; i = 1,2 \tag{14}$$

where θ denotes the convergence order and c represents the unknown constant to be determined. The convergence order for the rectangular port is 1.5432. The error norm and logarithmic error norm graph corresponding to the number of elements and the logarithmic value of number of elements is shown in Fig. 2. It is observed that the error norm graph and logarithmic error graph significantly decreases when the number of elements increases.

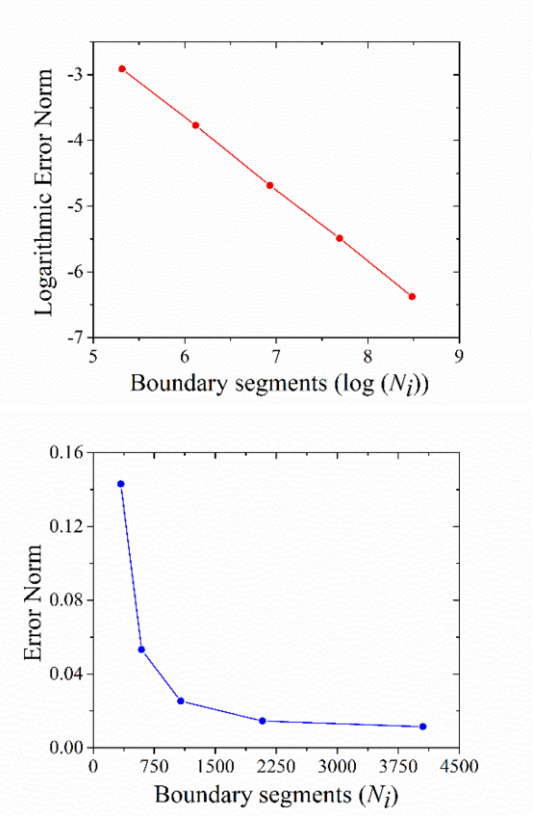

Figure 2. The convergence analysis with (a) Error norm and (b) Logarithmic error norm.

4. Numerical Validation

The numerical scheme that is discussed above is implemented on the rectangular port of length 0.31 m, breadth 0.06 m and its depth is 0.26 m to obtain numerical accuracy of the model. The response curve is obtained at the centre of the backwall (*P*) presented in the Fig. 3 to compare with the available experimental study of Ippen and Goda (1963) [2] and Lee (1971) [5] and with the analytical solutions. The two different resonance modes are obtained using the present numerical schemes, $k_1 = 1.32$ and $k_2 = 4.2$ which is similar to the previous schemes. On comparing with the available studies, it is concluded that present scheme shows good agreement with it and thus can be implement on complex geometry.

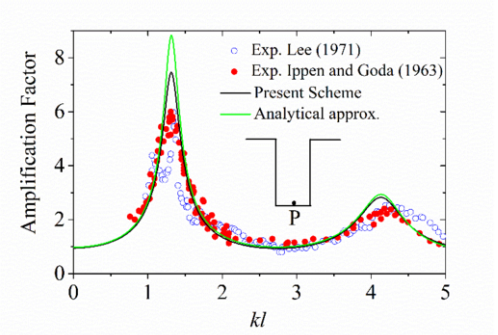

Figure 3. Comparison of simulations based on present technique with the analytical approximation and experimental data for rectangular port at backwall of the port 'P'.

5. Simulation Results

The spectral density utilized to examine the wave energy distribution with respect to wave periods or wave frequency. The current scheme is applied on Visakhapatnam port to evaluate the spectral density at four key locations within the port domain. The wave spectral density for the long wave is plotted against the wave period, which ranges from 30 s to 100 min with the difference of wave range 30 s at four record stations R_1 to R_4 is presented in Fig. 4. The different resonant modes are obtained for the different wave periods $T_1 = 2–3$ min, $T_2 = 6$-8 min, $T_3 = 18–19$ min and $T_4 = 70.5–80.5$ min respectively. It has been concluded that the distribution of waves energy depends on both the wave period and the position of the record points. The higher wave oscillations are generated in the Visakhapatnam port by the monochromatic waves when the wave approaches the coastal regions having wave periods in between T_1-T_4.

6. Conclusions and Discussion

The numerical model based on BEM is used to obtain the distribution of wave energy within the Visakhapatnam port. The convergence analysis is presented to present the accuracy of the model and the numerical simulation results are compared through wave amplification at the rectangular port and found valid with the experimental as well as

analytical approximations. Further the simulation results are obtained for the spectral density which provides the vital information about the wave energy distribution corresponding to the wave period for the different key locations outside and within the Visakhapatnam port are examined. At different wave intervals, the resonance modes in the spectral density plot are obtained.

The incoming waves which produces high amplification, are hazardous in the coastal regions and damages the coastal structures like moored vessels which lie in a port. The mentioned current numerical scheme is utilized to analyze the spectral density in the port; however, the practical physical prototype is very time consuming and expensive. The numerical model presented in the present paper is effectively and efficiently implemented on any arbitrary shaped port. The more accurate methods are required to achieve the higher precision, such as taking the breakwater concept and also including the nonlinearity concept to achieve a more accurate and authentic portrayal of realistic, dominant harbour conditions.

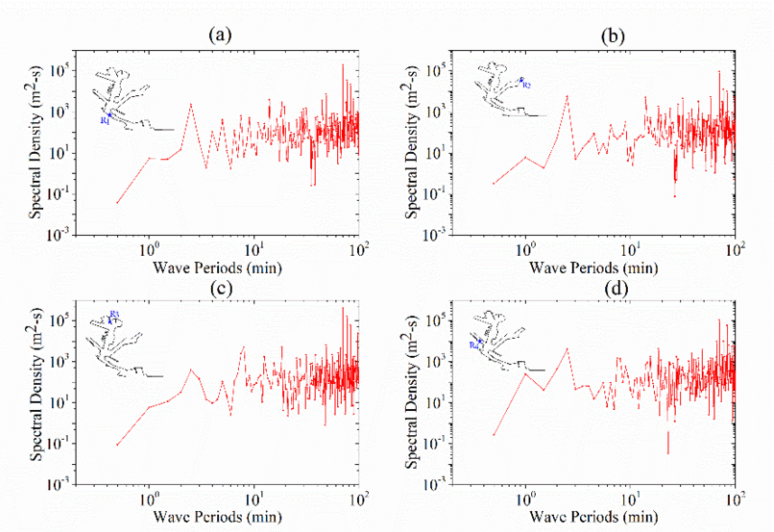

Figure 4. The analysis of wave spectral density for the record stations R1, R2, R3 and R4 within the Visakhapatnam port corresponding to the wave period ranging from 30 s to 100min having wave period difference 30 s.

Acknowledgement

The National Institute of Technology Delhi, Department of Applied Sciences (Mathematics) funded this research work.

References

[1] McNown JS. Wave and Seiche in Idealised Ports. In Gravity Wave symposium, National Bureau of Standards Circular. California, United States, University of California. 1952, Vol. 521, 153-164.

[2] Ippen AT, Goda Y. Waves induced oscillation in harbors: the solution for a rectangular harbor connected to the open sea. Report No. 59, Hydrodynamics Laboratory, MIT, (1963).

[3] Mei CC, and Ünlüata Ü: Resonant scattering by a harbor with two coupled basins. J. Eng. Math. 1976 Vol. 10(4), 333–353, doi: https://doi.org/10.1007/BF01535569
[4] Lomo P, Marcos M. Response of a harbor with two connected basins to incoming long waves. Appl. Ocean Res. 2006 Vol. 27, 209–215, doi: https://doi.org/10.1016/j.apor.2005.11.010
[5] Lee JJ. Wave-induced oscillations in harbours of arbitrary geometry. J. Fluid Mech. 1971 Vol. 45(2), 375–394, doi: https://doi.org/10.1017/S0022112071000090
[6] Lee HS, and Williams AN. Boundary element modeling of multidirectional random waves in a harbor with partially reflecting boundaries. Ocean Eng. 2002 Vol. 29(1), 39–58, doi: https://doi.org/10.1016/S0029-8018(01)00006-3
[7] Kumar P, Zhang H, and Kim KI. Spectral density analysis for wave characteristics in Pohang new harbor. Pure Appl. Geophys. 2014 Vol. 171(7), 1169–1185, doi: https://doi.org/10.1007/s00024-013-0710-x
[8] Kumar P, and Gulshan. Extreme Wave-Induced Oscillation in Paradip Port under the Resonance Conditions. Pure Appl. Geophys. 2017 Vol. 174(12), 4501–4516, doi: https://doi.org/10.1007/s00024-017-1646-3
[9] Kumar P, Rupali. Modeling of shallow water waves with variable bathymetry in an irregular domain by using hybrid finite element method. Ocean Eng. 2018 Vol. 165, 386-398, doi: https://doi.org/10.1016/j.oceaneng.2018.07.024
[10] Schmicker D, Duczek S, Liefold S, Gabbert U. Wave propagation analysis using high-order finite element methods: spurious oscillations excited by internal element eigenfrequencies. Tech. Mech. 2014 Vol. 34, 51–71, doi: https://doi.org/10.24352/UB.OVGU-2017-053
[11] Guerrini M, Bellotti G, Fan Y, and Franco L. Numerical modelling of long waves amplification at Marina di Carrara Harbour. Appl. Ocean Res. 2014 Vol. 48, 322–330, doi: https://doi.org/10.1016/j.apor.2014.10.002
[12] Dong G, Gao J, Ma X, Wang G, and Ma Y. Numerical study of low-frequency waves during harbor resonance. Ocean Eng. 2013 Vol. 68, 38–46, doi: https://doi.org/10.1016/j.oceaneng.2013.04.020
[13] Gao J, Ji C, Gaidai O, and Liu Y. Numerical study of infragravity waves amplification during harbor resonance. Ocean Eng. 2016 Vol. 116, 90–100, doi: https://doi.org/10.1016/j.oceaneng.2016.02.032
[14] Gao J, Ji C, Liu Y, Ma X, and Gaidai O. Influence of offshore topography on the amplification of infragravity oscillations within a harbor. Appl. Ocean Res. 2017 Vol. 65, 129–141, doi: https://doi.org/10.1016/j.apor.2017.04.001
[15] Gao J, Zhou X, Zhou L, Zang J, and Chen H. Numerical investigation on effects of fringing reefs on low-frequency oscillations within a harbor. Ocean Eng. 2019 Vol. 172, 86-95, doi: https://doi.org/10.1016/j.oceaneng.2018.11.048
[16] Xing X. Computer Modeling for Wave Oscillation Problems in Harbors and Coastal Regions. Ph. D. thesis, Univ. Southern California, Los Angeles, California, (2009).
[17] Maa JP, Tsai C, Juang W, and Tseng H. A preliminary study on Typhoon Tim induced resonance Hualien Harbor, Taiwan. Ocean Dyn. 2011 Vol. 61, 411–423, doi: https://doi.org/10.1007/s10236-010-0355-6
[18] Lopez M, Iglesias G, and Kobayashi N. Long period oscillations and tidal level in the Port of Ferrol. Appl. Ocean Res. 2012 Vol. 38, 126–134. https://doi.org10.1016/j.apor.2012.07.006
[19] Dong G, Zheng Z, Ma X, and Huang X. Characteristics of low-frequency oscillations in the Hambantota Port during the southwest monsoon. Ocean Eng. 2020 Vol. 208. https://doi.org/10.1016/j.oceaneng.2020.107408
[20] Mitsuyasu H. On growth of spectrum of wind generated waves (2)–spectral shape of wind waves at finite fetch. In: Proc 17th Japanese conf on coastal engineering. Tokyo (Japan); ASCE; 1970. p. 1–7.